Structural evolutions of spinels under ions irradiations

D. Gosset[a,*], D. Simeone[a], M. Dutheil[a], G. Baldinozzi[b], S. Bouffard[c], M. Beauvy[d]

[a]CEA Saclay, bat. 453 ; DMN/SRMA/LA2M ; F-91191 Gif/Yvette Cedex, France,

[b]G. Baldinozzi, LPMS, UMR CNRS 8580, ECP, F-92295 Chatenay-Malabry cedex, France

[c]CIRIL-GANIL, BP 5133, F-14070 CAEN Cedex 5, France,

[d]DEC, CEA Cadarache, 13108 St Paul-lez-Durance cedex, France

* coresponding author, e-mail dgosset@cea.fr

1 Introduction

In the frame of the nuclear wastes management French policy, a possible way to reduce the minor actinides (Np, Am, Cm) volume to be stored for long duration is selective burning (i.e. transmutation in short decay period elements) in dedicated reactors. This requires the use of 'neutronically' inert matrix materials to dilute the actinide to be burned and retain the fission products. Among the possible materials, spinel $MgAl_2O_4$ has been extensively studied, thanks to good chemical inertness, high temperature resistance and good neutron irradiation resistance.[1, 2] However, the studies have shown swelling of the material and amorphisation for the highest fluences. Prior to this amorphisation, drastic structural modifications have been observed some authors have interpreted as a crystalline phase transformation.[3, 4] On the other hand, there is no clear evidence for the formation of extended defects such as dislocation loops or networks.[5]

As inert matrix, those materials will be submitted to irradiations of different origins: fast neutrons, α particles (~ 6 MeV) and recoil atoms (~ 240 uma, 100 keV) from natural actinides α-decay, fission products (~ 80-150 amu, ~ 70-100 MeV), leading to different damage processes (resp. small or large displacement cascades, electronic interactions). Simulating the resulting damages then requires the use of different ion irradiations (resp. light and heavy slow ions, swift heavy ions).

$MgAl_2O_4$ is part of the spinel family with general formula AB_2O_4 and $Fd\bar{3}m$ space group. Divalent A and trivalent B cations are respectively located on the tetrahedral 8a and octahedral 16d Wyckoff positions, sharing O atoms located on the 32e sites. Due to cationic radii effects, O atoms are slightly shifted from the (¼,¼,¼) position to a (u,u,u) more general one, leading to octahedral and tetrahedral distortions. Most of the possible cationic sites are empty: 16c

(octahedral), 8b and 48f (tetrahedral). Synthetic materials differ from this ideal scheme and are characterised by a partial inversion of the A and B atoms, mainly depending on the elaboration conditions.

In order to improve the description of the first damage steps of spinels, we have performed swift heavy ions irradiations in GANIL: the main advantage of such an irradiation is the large nearly homogeneously damaged volume (thickness around 20-40 μm). We have then performed X-Ray analysis of the damaged areas. The major drawback of such an analysis in the case of $MgAl_2O_4$ spinel is the poor sensitivity to the cations distribution, due to their low atomic mass difference. We have then performed the same analysis on equivalent materials $ZnAl_2O_4$ [6] and $MgCr_2O_4$. On the other hand, we have performed Raman analysis in order to determine the actual local crystal symmetry. In this paper, we confirm that the initial $Fd\bar{3}m$ space group is not changed during irradiation [7], but the unit cell shows apparent drastical changes with high cationic inversion rates and the occupation of normally empty sites, this depending on the material composition. Moreover, subsequent isochronal annealings show different healing processes in the three materials.

2 Experimental

$MgAl_2O_4$ powder produced by Bailowsky company containing 1.2% MgO and 0.3% Al_2O_3 was hot-pressed (1 hour, 1923 K, 300 MPa under H_2 atmosphere)leading to high density (98% theoretical density), low grain size (3μm) pellets. High purity ZnO and Al_2O_3 powders were calcinated 1 hour at 1473 K and sintered 8 hours at 1800 K to produced $ZnAl_2O_4$ low density (67 % theoretical density) pellets. [6]. High purity MgO and Cr_2O_3 (Alfa-Aesar) powders were blended and pressed (300 MPa) prior to sintering (1 day at 1200 K) resulting in low density (75 %) $MgCr_2O_4$ pellets. All pellets were then sieved and polished.

X-ray analysis were performed with INEL CPS120 curved position sensitive detectors, during ion irradiations at GANIL and prior irradiations and after each isochronal annealings. The GANIL facility allows quick spectra collection, but with a poor sensitivity (spectra practically limited to the 20-80° 2θ range, graphite monochromator selecting $CuK\alpha_{1+2}$ line). All other spectra (prior and after irradiations, after isochronal annealings) were collected on a second facility with much better optical performances [8] (parallel $CuK\alpha_1$ monochromatic incident beam with low equatorial divergence (Sollers slits), 0-120° 2θ range) and high signal/noise ratio. The refinement of the X-ray diffraction diagrams were performed with the XND Rietveld program [9].

The Raman spectra of irradiated samples were recorded in a back-scattering configuration under microscope, with a T64000 Jobin-Yvon spectrometer with a CCD detector. A confocal hole was adjusted to enhance the signal coming from the surface. To avoid the luminescence signal due to impurities, the 514.5 and 488 nm excitation laser lines were used.

The irradiations were performed at GANIL (Grand Accélérateur National d'Ions Lourds at Caen) with 820 MeV Kr ions at room temperature and a constant flux (10^9 cm^{-2} s^{-1}). The slowing down of the ions (8 to 12 keV/nm, estimations with SRIM-2000 [10]) in the zone analysed with X-ray diffraction (thickness around 20 μm) is then purely due to electronic interactions, the contributions of direct displacement cascades can be practically neglected. The fluences range from 10^{13} to 10^{15} cm^{-2}.

3 Results and interpretation

First of all, we observed that the diffraction diagrams show the same evolution during irradiation than already observed in quite different irradiation conditions. On Fig. 1, we have reported the diffraction diagrams of $MgAl_2O_4$ prior and after irradiation: the same modifications as stated by Sickafus et al. [3, 4] are observed: disappearing of all the (hkl) but the (4h,4k,4l) lines, partial amorphisation for the highest fluences. The same observation can be done when comparing the results obtained by Chukalkin *et al.* when irradiating $MgCr_2O_4$ [11]. However, in the first case the material was irradiated with 400 keV Xe ions at low temperature (20 K) and in the second case, the material was irradiated by neutrons (fast neutrons 2.10^{20} cm^{-2}, E > 1MeV) around 50°C. At last, irradiations of $ZnAl_2O_4$ with slow heavy ions show the same evolution of the X-ray diagrams [12] than we observe here. As a consequence, the structural modifications induced by irradiations in the spinels we consider here do not depend on the damage mechanisms: electronic slowing-down and subsequent energy transfer to the structure ions in the case of swift heavy ions, large displacement cascades in the case of slow heavy ions and small displacement cascades in the case of fast neutrons. This is of primary importance since it allows the comparison of different experiments.

The second key result is the unambiguous identification of the cell structure of the materials. From TEM observations or X-ray analysis, analogous to the results reported in Fig. 1, many authors assumed that the disappearing of the odd (hkl) lines should be attributed to a cell modification, from $Fd\bar{3}m$ to fcc $Fm\bar{3}m$, together with a cell parameter divided by 2: such a structure can indeed lead to the right diffraction diagram. To check this point, we have performed Raman analysis on $MgAl_2O_4$ prior and after irradiation. The result (Fig. 2) clearly shows that the structure is not modified since all the

characteristic lines of the $Fd\bar{3}m$ space group remain visible after irradiation, even when the rock salt $Fm\bar{3}m$ space group would show only one line.

We have then performed Rietveld analysis of the X-ray diffraction diagrams. The results are summarized in table 1. In the case of $ZnAl_2O_4$, all the diagrams could be accounted assuming an increase of the classical Zn-Al inversion ratio, with an exponential-like behaviour with the fluence. In the case of $MgAl_2O_4$, we first try to simulate the diffraction diagrams assuming again an increase of the inversion ratio. On the other hand, the atomic diffusion factors of Mg and Al are so close they can hardly be distinguished by X-ray diffraction: we then defined a virtual 'Mg+Al' atom with a 'mean' atomic diffusion factor. This allows a correct simulation of the diagram of the most irradiated samples[7]. However, considering the influence of the occupancies of the different sites to the actual relative intensities of the different (hkl) lines (table 2) leads us to assume that the cations, beyond the classical inversion, were also partially distributed on normally empty (forbidden) sites (table 1). On the other hand, the oxygen sub-network is little affected, we mainly observed an increase of its Debye-Lorentz coefficient (apparent thermal agitation or poor localisation) and a oxygen atomic position (u) shift lower than 1 % The same structural modifications had also to be assumed to analyse the $MgCr_2O_4$ X-ray diagrams. In this case, thanks to the cation masses difference, the sensitivity of the analysis is much better.

The first question which arises here is then the way the structure can accommodate such modifications. Since the cations can hardly be located on neighbour sites, due to strong Coulombian repulsion, medium-range reorganisation processes are to be activated. From re-examination of previously published high resolution TEM observations[13], we may assume that reordering of the structure leads to the formation of nano-sized domains with normal sites occupations (including inversion) separated by partial stacking faults, this allowing the long-range conservation of the oxygen sub-network we observe. Using X-ray diffraction (long-range analysis) or Raman spectroscopy (local symmetry), such a nanostructured material could not be differentiated from a homogeneous material with a mixing on 8a, 16c, 16d and 48f sites.

In order to improve the description of the irradiation damages, we then performed X-ray diffraction analysis after isochronal annealings (30 mn, 50°C steps). Preliminary results are summarized in Fig. 3 in which we have reported the

evolution of the most sensitive parameters, i.e. the cell parameter (a) and the oxygen position (u). The behaviour of the materials are very different. The material which has the most simple behaviour, $ZnAl_2O_4$, shows a healing in a single, narrow stage around 850 K. $MgAl_2O_4$ shows two well-separated stages, around 520 and 870 K. At last, $MgCr_2O_4$ shows a large stage around 850 K, with a possible first small stage around 720 K. This last result is in good agreement with Chukalkin *et al.*[11], who have shown that the intensities of the diffraction lines of $MgCr_2O_4$ irradiated with neutrons recover in the same temperature stages, the relative heights of the stages depending on the (hkl)'s. From these results, we may assume that in the 'complex' $MgAl_2O_4$ and $MgCr_2O_4$ materials, the abnormal sites occupancies (first stage) and the inversion rates (second stage, around 850 K) recover in different temperature ranges.

4 Conclusion

Different spinels materials have been irradiated with swift heavy ions. The results show that the resulting damages do not depend on the basic irradiation mechanisms. On the other hand, Raman spectroscopy shows that the crystal structure is unaffected and remains $Fd\bar{3}m$. However, in the case of $MgAl_2O_4$ and $MgCr_2O_4$, the irradiation leads to the classical cation inversion, as in $ZnAl_2O_4$, but also to the occupancy of normally empty sites. At last, isochronal annealings show a more complex behaviour for these two Mg-materials.

Analysis of the diffraction diagrams are in progress. The main questions which now arise are the actual defects structure (occupancy of forbidden sites) in these materials, the scaling of the effects of different impinging particles, the way the global structure accommodates these defects and the parameters controlling the sensitivity to the materials composition. As a matter, this could help determining a better inert matrix material with improved irradiation resistance.

Acknowledgements

We are very indebted to P. Daniel (LPEC, UPRES A CNRS 6087, F-72085 Le Mans) who performed the Raman analysis.

References

.1. G. Summers, G. White, K. Lee, J. Crawford, Phys. Rev. B 21(6) (1980) 2578.

. 2. K.E. Sickafus, A.C. Larson, N. Yu, M. Nastasi, G.W. Hollenberg, F.A. Garner, J. Nucl. Mater. 219(1-3), (1995), 128-134

. 3. R. Devanathan, K. Sickafus, M. Nastasi, Phil. Mag. Lett. 72(3) (1995) 155.

. 4. M. Ishimaru, I. Afanassiev-Charkin, K. Sickafus, Appl. Phys. Lett. 76(18) (2000) 2556.

. 5. C. Kinoshita, K. Fukumoto, K. Fukuda, F. Garner, G. Hollenberg, J. Nucl. Mater. 219 (1995) 143.

. 6. C. Dodane-Thiriet, Ph-D thesis 6814, Orsay, Paris-XI university (2002)

. 7. D. Simeone, C. Dodane-Thiriet, D. Gosset, P. Daniel, M. Beauvy, J. Nucl. Mater. 300 (2002) 151-160

. 8. D. Simeone, D. Gosset, J.L. Bechade, CEA-R 5975 report (2001)

. 9. J.F. Berar, G. Baldinozzi, CPD Newsletter 20 (1998) 3

. 10. J. Ziegler, http://www.srim.org/

. 11. Y. Chukalkin, V. Petrov, V. Shtirts, B. Goshitskii, Phys. Stat. Sol. A92 (1985) 347

. 12. D. Simeone, G. Baldinozzi, D. Gosset, M. Dutheil, S. Bouffard, to be published.

. 13. L. M. Wang, S. X. Wang, J. Lian, R. C. Ewing, , A. Arbor, 1st Annual Michigan Materials Research Symposium (MMRS), May 5 - 6, 1999

captions

Fig. 1: X-ray diffraction pattern of $MgAl_2O_4$ prior (bottom) and after (top) ion irradiation: only the (4h, 4k, 4l) lines remain

Fig. 2. Raman spectra of non- (top) and irradiated spinel $MgAl_2O_4$. Dotted lines: Fd3m characteristic lines. Shaded areas: contribution of amorphous material

Fig. 3: isochronal annealings of irradiated spinels versus annealing temperature (K). Top: $ZnAl_2O_4$, middle: $MgCr_2O_4$, bottom: $MgAl_2O_4$. Left: position of 32e site (O), right: cell parameter (Å)

table 1. Structural modifications of the spinels after 820 MeV Kr irradiation

table 2: relative intensities of (hkl) lines (real and imaginary parts of the structure factor) as a function of the occupancies of the different sites (resp. A for 8a, C for 16c, etc.)

figure 1

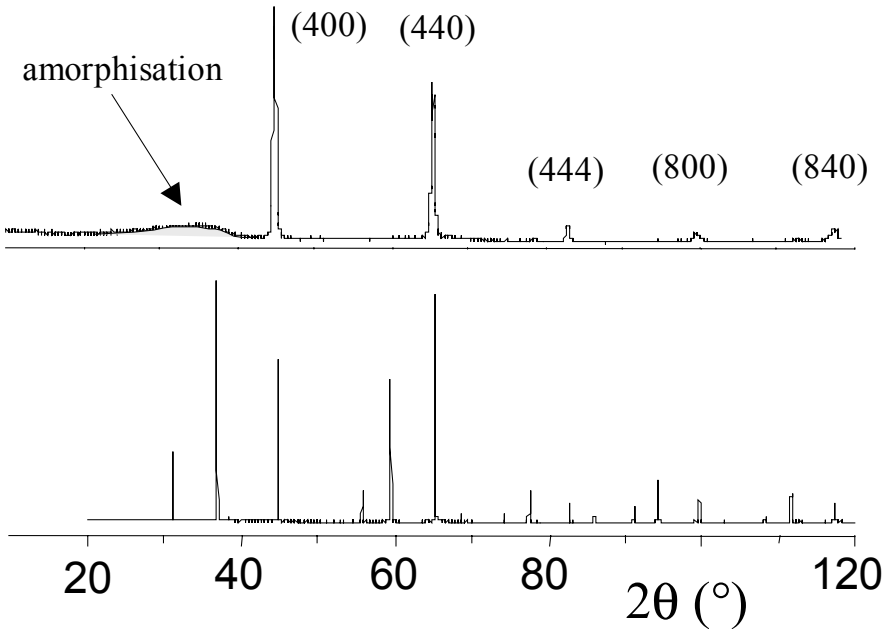

figure 2

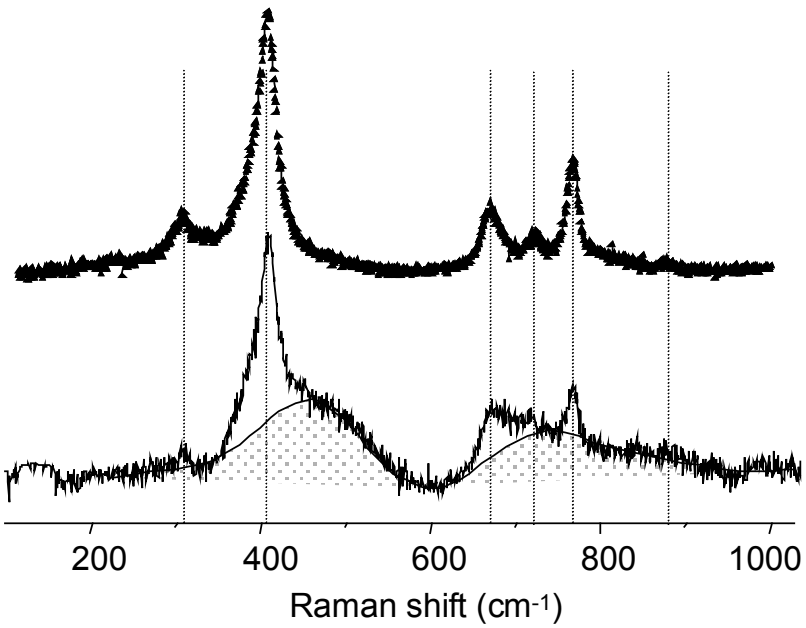

figure 3

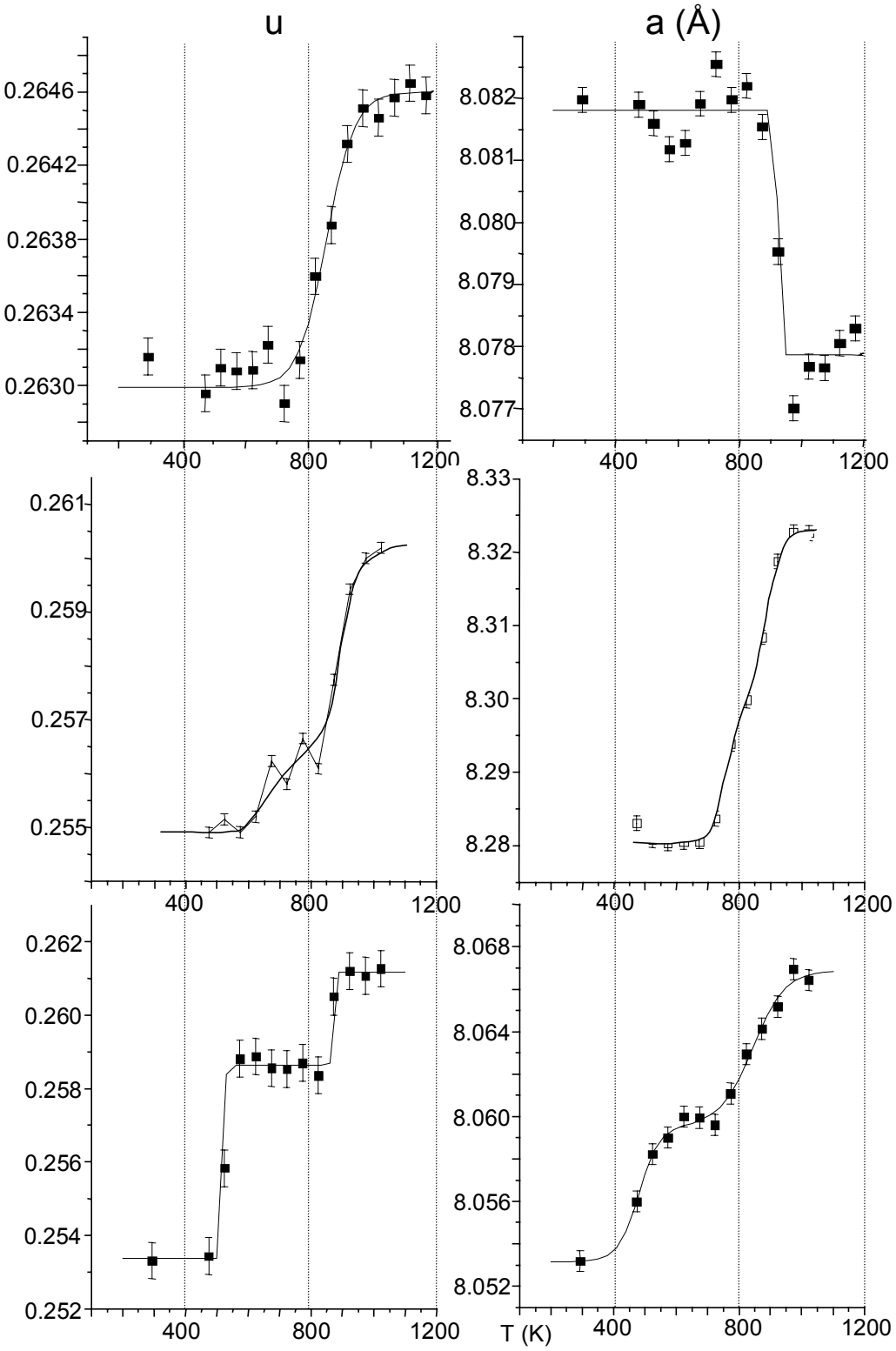
u
a (Å)
0.2646
0.2642
0.2638
0.2634
0.2630
8.082
8.081
8.080
8.079
8.078
8.077
400
800
1200
0.261
0.259
0.257
0.255
8.33
8.32
8.31
8.30
8.29
8.28
0.262
0.260
0.258
0.256
0.254
0.252
8.068
8.064
8.060
8.056
8.052
T (K)

table 1

site	$ZnAl_2O_4$				$MgAl_2O_4$				$MgCrI_2O_4$			
	initial		irr. 7.6 10^{12}		initial		irr. 9.3 10^{12}		initial		irr. 3.8 10^{12}	
	Zn	Al	Zn	Al	Mg	Al	Mg	Al	Mg	Cr	Mg	Cr
8a	0.91	0.09	0.72	0.28	1.00		0.67		1.00		0.44	
8b												
48f							0.25				0.42	
16c							0.09	0.25			0.14	0.67
16d	0.09	1.91	0.28	1.72		1.87		1.62		1.92		1.26
u	0.264		0.262		0.261		0.257		0.260		0.252	
a (Å)	8.081		8.090		8.069		8.066		8.332		8.299	

Table 2

(hkl)	Re	Im
(440) (800)	[8(A+B) + 48F] + [16(C+D)]	0
(400) (444) (840)	[8(A+B) + 48F] – [16(C+D)]	0
(222) (422) (620) (642)	8(A+B) – 16F	0
(222) (622) (662)	0	–16(C+D)
(111) (331)	4(A-B) + 4√2(C-D)	–Re
(311) (333)	4(A-B) – 4√2(C-D)	Re
(511)	4(A-B) – 4√2(C-D)	–Re
(531)	4(A-B) + 4√2(C-D)	Re